Journal of Physics and Chemistry of Solids 138 (2020) 109268

Contents lists available at ScienceDirect

Journal of Physics and Chemistry of Solids

journal homepage: http://www.elsevier.com/locate/jpcs

PDMS packaged microfiber knot resonator used for sensing longitudinal load change

Lu Cai [a], Jin Li [a,b,*]

[a] College of Information Science and Engineering, Northeastern University, Shenyang, 110819, China
[b] State Key Laboratory of Applied Optics, Changchun Institute of Optics, Fine Mechanics and Physics, Chinese Academy of Sciences, Changchun, 130033, China

ARTICLE INFO

Keywords:
Microfiber knot resonator
Microfiber sensor
Load sensor
Integrated optics
Fiber optics

ABSTRACT

In this paper, we proposed a sensitive load sensor probe based on microfiber resonator. The microfiber was prepared from the common single mode fiber by one-step heating-stretching method and used to fabricate a microfiber knot resonator (MKR) by micromanipulation technique. This MKR was packaged later by polydimethylsiloxane (PDMS) film layer in two glass slides. The load sensing performance have been explored and compared for the bare MKR structure and PDMS packaged MKR probe. The longitudinal load sensing characteristics were experimentally demonstrated with a small sensitivity of 6 p.m./N, due to the large Young's modulus and low elasto–optical effect of silica materials. In order to increase the longitudinal load sensitivity and stability of bare MKR, we chose PDMS to encapsulate MKR due to its small Young's modulus and large Poisson's ratio. The strain sensing performance of both a bare and PDMS packaged silica MKR were experimentally demonstrated and compared. The experiment results revealed a sensitivity of 94.5 p.m./N. The simple structure, low loss and easily fabrication process pave its way to a miniature strain sensor chip.

1. Introduction

In recent years, micro–nano optical fiber (MNF) sensing technology has been widely concerned due to its excellent sensing and mechanical performance [1–3]. Various ring resonators have been constructed from the flexible MNF [4], and demonstrated with the ignorable polarization effect for sensing application [5]. The ring resonators based on ring, loop, knot and muti–loops have been reported recently to measure temperature, humidity, refractive index, acceleration, strain, gas concentration, etc. [6–9]. The MNF knot ring (MKR) temperature sensor was experimentally demonstrated with a sensitivity of 280 p.m./°C in the range of 28–140 °C [10]. Wu et al. compared the temperature sensing characteristics of silica and polymer MKR, whose sensitivities reached up to 52 p.m./°C and 266 p.m./°C, respectively, with a response time of less than 1 ms and 5 ms, respectively [11]. The maximum refractive index sensitivity for a bare polymer MKR is 95.5 nm/RIU [12]. By cascading the MKRs and introducing into the "cursor effect", Xu et al. broadened the free spectral range (FSR) of the output spectrum, thereby increased the corresponding sensitivity up to 6523 nm/RIU [13]. A humidity sensor probe based on silica and polymer MKRs was demonstrated with a sensitivity of 88 p.m./RH [14]. This sensitivity has been further improved to 53.7 p.m./RH during 30 %RH–50 %RH by Ahmed et al. Where, the MKR structure has been coated by the single–layer graphene oxide film due to its high permeability and high stability in water. In addition, MKR sensors have also been proposed as an ultraviolet radiation detector by elaborating a thin layer of polymer PAni [15]. Under the irradiation of UV light, the sensitivity was measured as 6.61 nm/(W · cm^{-2}) [16]; Azlan et al. designed and experimentally demonstrated an MKR–based current sensor [17]. Where, a straight copper wire was placed against with the MKR, a current sensitivity of 700 p.m./A^2 was obtained in the working range of 0–2 A. Based on the unique electrical and optical properties of graphene, the sensitivity of the MKR current sensor was experimentally demonstrated with 67.297 μm/A^2 [18]. To explore the mechanical response, a hybrid plasmonic MKR was demonstrated with a pressure sensitivity of 9.34 p.m./kPa and a vibration response in the range of Hz to kHz [19]. The similar MKR accelerometer was reported by covering the MKR with Efron PC-373 and demonstrated with a sensitivity of 654 mV/g [20]. MKR was also used to measure the acoustic wavefield with the sensitivity of 5.83 p.m./mPa [21].

In the previous paper, we proposed a polydimethylsiloxane (PDMS) packaged MKR sheet and studied its temperature sensing performance

* Corresponding author. College of Information Science and Engineering, Northeastern University, Shenyang, 110819, China.
E-mail addresses: cailu@neuq.edu.cn (L. Cai), lijin@ise.neu.edu.cn, mengfanli@ise.neu.edu.cn (J. Li).

https://doi.org/10.1016/j.jpcs.2019.109268
Received 4 October 2019; Received in revised form 8 November 2019; Accepted 9 November 2019
Available online 9 November 2019

[22,23]. Based on the unique properties of MKR and PDMS, a load sensing probe was proposed and experimentally demonstrated later [24]. The contribution of PDMS on the load sensing performance will be further discussed in this paper. The proposed structure was easy to prepare and low-cost. It can convert the longitudinal load into its deformation in the ring length. In contact sensing, temperature and load need to be considered simultaneously in many applications. That is why the temperature and load sensing performance for the proposed MKR structure is explored in different works. Ultra-thin film-type structure is conducive to its application in narrow areas.

2. MNF and MKR preparation

The MNF with uniform diameter and smooth surface has been fabricated by self-adjusting flame stretching technique. Firstly, the normal single mode fiber (SMF) in the length of ~10 cm was cut, whose coating layer in a length of ~2 cm was removed and uniformly heated on one Bunsen burner. The melted section was stretched on the both ends of SMF to obtain the MNF with the desired diameter among 2 μm–~10 μm. Following above method, the MNF with a diameter of 6.92 μm and length of 2 cm was prepared by flame heating–stretching method, as shown in Fig. 1(a–c). To prepare the MKR structure, the double-tapered SMF was cut in middle section. The micrograph of one end of MNF with uniform diameter was shown in Fig. 1 (a). In the simulation mode (Comsol software), the MNF (refractive index: 1.4679) was coated by one layer of PDMS (refractive index: 1.4). Due to the little refractive index difference, when light transmits along the MNF, most of them will be confined in the fiber core, and some will goes along the MNF surface in the form of evanescent wave. The taper region diameter decreased significantly in the length of dozens of micrometers, as shown in Fig. 1 (b). However, the MNF section has the uniform diameter, as compared with SMF in Fig. 1(c), which will be used to prepare the MKR structure.

The optical fiber probe was used to perform the knotting operation under an optical microscope to fabricate an MKR with a micro–ring diameter of 6 mm. Fig. 1(d–f) showing the fabrication process of MKR. One end of MNF was circled firstly (Fig. 1(d)); The two segments of MNF naturally lapped together due to electrostatic forces and van der Waals forces (Fig. 1(e)); Then, the MNF was held at one end and the other end was reversed through the ring, similar to the needle-threading. By stretching horizontally the both ends of MNF, a junction naturally formed at the coupling location, as shown in Fig. 1(f). There are the following precautions in the preparation of MKR, for examples, the tiny size of MNF are susceptible to air flow; the surface of MNF is extremely easy to adsorb microscopic particles in air due to the electrostatic force and van der Waals force. Therefore, the stability and cleanness of air environment should be seriously controlled.

3. Theoretical analysis of transverse load

Firstly, a MKR was fabricated, with the ring diameter of 6.0 mm and the MNF diameter of 6.92 μm. The load sensing performance was experimentally demonstrated with a sensitivity of 6 p.m./N. To improve the stability and sensing performance, we fabricated another MKR with the microfiber diameter of 7.20 μm and ring diameter of 4.0 mm, encapsulated it with PDMS and packaged it using two glass slides, as shown in Fig. 2. Where, the length, width and thickness of the glass slides were 7.6 cm, 2.6 cm and 1.0 mm, respectively; the thickness of PDMS was less than 0.5 mm. The microscope pictures for the fiber taper and knot ring sections of the MKR structure were illustrated in the insets of Fig. 2.

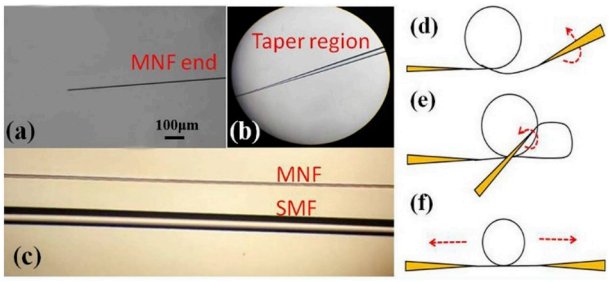

Fig. 1. Microscope images of (a) uniform end and (b) taper region of MNF, as well as (c) its size comparing with SMF; Fabrication process of MKR includes (d) circling, (e) inserting and (f) stretching.

The prepared MKR was then packaged by the PDMS film with the excellent elastic properties with the Young's modulus $E_p = 750$ KPa (compared to that of silica $E_s = 72$ GPa) and Poisson's ratio $\eta = 0.45$. The small Young's modulus makes it easy to be deformed under a certain force. A large Poisson's ratio promises the longitudinal load converting to transverse strain, which in turn makes the MKR more sensitive to axial stress and implements the transverse load sensors with high sensitivity. Due to the large Poisson's ratio of PDMS, the deformation caused by the transverse loading of MKR would be ignored. The load measurement diagram is shown in Fig. 2. When the PDMS film layer is subjected to transverse pressure F_z in the z-direction, it will undergo the expansion in both x-axis and y-axis and the contraction in z-axis. When the influence of MKR is ignored, according to Hooke's law, the strain of PDMS in the x-axis direction is [25]:here, the transverse compression area is $A_{p(xy)}$, which also refers to the microring area of MKR. When PDMS expands on the x-axis and y-axis, it interacts with the MKR and reduces the deformation of itself and increases the axial strain of MKR. The interaction is represented by F_f. The PDMS and MKR are exerted on the same load intensity on the x-axis and y-axis:

$$\varepsilon = \varepsilon_{ff} = \varepsilon_p - \varepsilon_{pf} \tag{2}$$

Where in, ε_{ff} is the increasing axial load of the MKR under the interaction force F_f, and ε_{pf} indicates the decreasing load of the PDMS under the interaction force F_f. Therefore, the interaction force can be further expressed as:

$$F_f = \int_0^{\pi D} 2\pi r E_s \varepsilon_{sf} dR = A_{p(yz)} E_p \varepsilon_{pf} \tag{3}$$

Among them, E_s is the Young's modulus of the silica MNF, E_p is the Young's modulus of PDMS, and $A_{p(yz)}$ is the cross-sectional area of PDMS in the x-axis direction. The transverse load of the MKR caused by the longitudinal strain is

$$\varepsilon_{fx} = \varepsilon_{ff} = \eta F_z \frac{A_{p(yz)}}{A_{p(xy)}\left(A_{p(yz)}E_p + 2\pi^2 r D E_s\right)} \tag{4}$$

where, D is the microring diameter of MKR and R is the radius of MNF. Therefore, the strain in the unit transverse load can be expressed as:

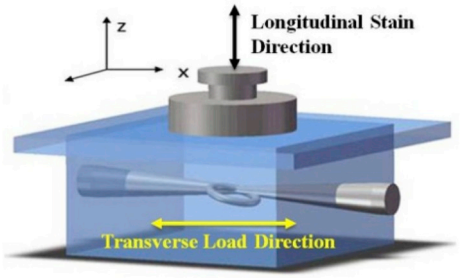

Fig. 2. Load measure schematic of PDMS packaged MKR.

$$\varepsilon_p = \eta \frac{F_z}{A_{p(xy)}E_p} \tag{1}$$

$$k_F = \frac{\varepsilon_{fx}}{F_z} = \eta \frac{A_{p(yz)}}{A_{p(xy)}\left(A_{p(yz)}E_p + 2\pi^2 r D E_s\right)} \quad (5)$$

4. Transverse load sensing experiment of bare MKR

As shown in Figs. 2 and 3 (c), the MKR was encapsulated by PDMS between two slides. End fibers of MKR were protected by Poly tetra fluoroethylene (PTFE) tube. This packaging method has the following characteristics: 1. The sensing area of MKR is fixed; 2. The transverse load can be distributed uniformly and effect on the PDMS film and MKR structure; 3. The thickness of PDMS film would be exactly controlled by the diameter of PTFE, which ensures a constant thickness for the following different sensor probes. The amplify stimulated emission (ASE) with the wavelength ranging from 1520 nm to 1560 nm was used as the light source. The optical spectrum analyzer (OSA, AQ6370) was used to analyze the output spectrum and a digital push-pull force meter (SH-500) was used to exert the longitudinal load with a minimum resolution of 0.001 N and maximum force of 500 N.

Fig. 3 (b) indicates the microscope image of the knot location of MKR. When it is compressed, the refractive index of the fiber along the load direction will change due to the elasto–optical effect. The greater elasto–optical coefficient will result in better mechanical strain sensitivity; furthermore, the micro-ring length will also change as a function of the external force. The changes in either micro-ring length or effective refractive index will cause the linearly drift of the output spectrum. Therefore the longitudinal load can be obtained by demodulating the wavelength shift of the output spectrum. Due to the fast sensing response time in the experiment, the temperature was assumed as a constant during the longitudinal load measurement. The corresponding output spectrum was recorded and shown in Fig. 4. However, the interference effect between the fiber core mode and the evanescent field mode dominates in this MKR structure, because the microfiber diameter is not thin enough in this work. Therefore, the interference (resonance) is different with a common ring resonator (sharp resonance peaks) (see Fig. 5).

It can be seen from Fig. 4 that as the longitudinal load increases to 5 N, the resonant wavelength blue-shifted from 1550.740 nm to 1550.704 nm. The longitudinal load sensitivity and the resolution were calculated as 7 p.m./N and 2.86 N, respectively. When the load increased from 0 N to 5 N, the average sensitivity was determined from the wavelength shift value. Indeed, it is impossible to distinguish the wavelength shift for a bare MKR when the load change is < 3 N due to the resolution of OSA. Since the large Young's modulus of silica is 72 GPa, the external load force won't significantly deform the corresponding structures. Only a slightly shift of the resonance wavelength was observed in the output spectrum. Once being loaded, the diametral compression of the bare fiber will result in the structural reshape and

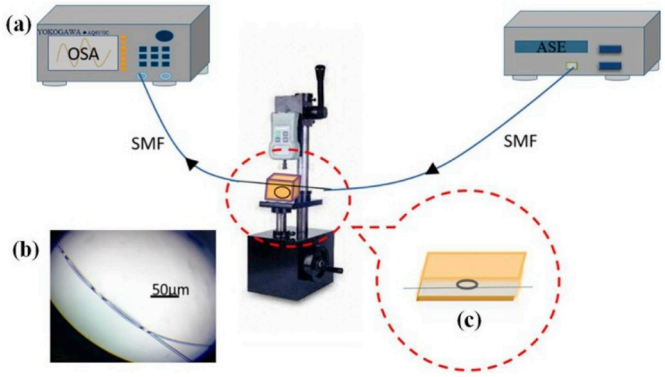

Fig. 3. (a) Schematic diagram of longitudinal load sensing experiment based on MKR; (b) microscope image of knot area; (c) schematic of PDMS packaged MKR.

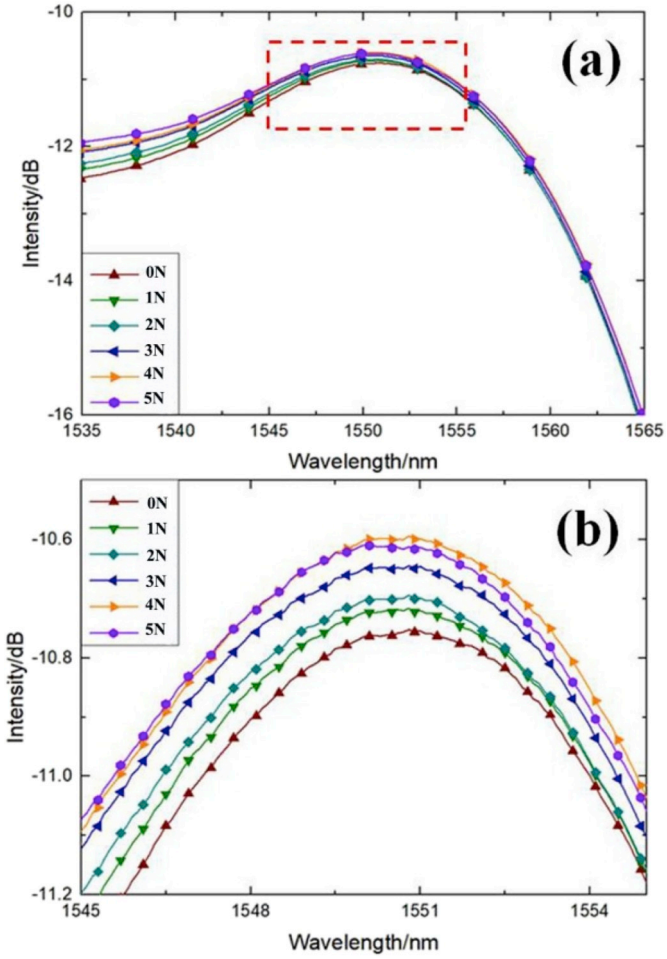

Fig. 4. (a) Transmission spectra of MKR with longitudinal load increasing and (b) enlarge part (red-dot square) near resonance peaks.

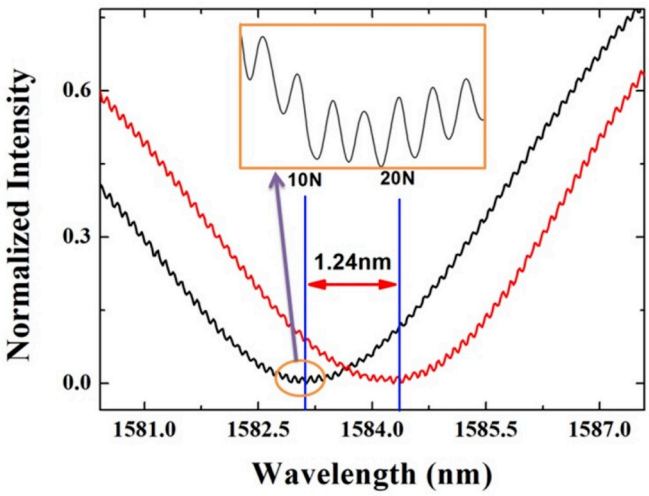

Fig. 5. Resonance dips red-shifted for 1.24 nm when the longitudinal load increased from 10 N to 20 N. Inset shows the enlarge section of one dip with muti-peaks.

light intensity change [26], which will differ from the structures geometry and fiber materials.

Compared to other fiber-optic sensing methods (such as fiber interferometers [27–29]), the sensitivity of the load force is still low for

the bare MKR, and the bare silica microfiber is fragile. Indeed, for the microfiber resonators with the fiber diameter of several micrometers, the transmission light is divided into two parts: fiber core part and fiber surface part, which will interference with each other at the taper region. The double-tapered microfiber plays as a Mach-Zenhder interferometer. When the microfiber was knotted into a ring, the Mach-Zenhder interference peaks (with wide FSR) and ring interference peaks (with narrow FSR) will overlap together [30]. The intensity of the ring interference peaks is very weak for the microfiber with bigger diameter.

5. Load sensing performance of PDMS packaged MKR

To package the MKR as an independent sensor probe, we chose PDMS to encapsulate MKR due to its small Young's modulus and large Poisson's ratio. The MKR was prepared based on the foregoing manufacturing method. Its two ends were connected with two normal single mode fiber and connected with the ASE light source and the OSA, respectively. As shown in Fig. 3(c), the MKR was firstly packaged by the PDMS film (gray part) and then covered by two slide glasses with a length of 7.6 cm and width of 2.6 cm (yellow part). When the longitudinal load increases, due to the small Young's modulus of PDMS, it is prone to be deformed and leads to the change of the ring length of MKR, which will finally causes the shift of the resonance peak in the transmission spectrum. The wavelength vibration as a function of the measured longitudinal load will be obtained by the wavelength demodulation method. The diameter of the MNF prepared in the experiment was 7.2 μm, the diameter of the micro-ring was 4 mm, and the thickness of the entire PDMS-packaged MKR was less than 0.5 mm.

When the longitudinal load increased from 10 N to 20 N, the resonance dips with muti-peaks turned out due to the microfiber loop resonator. A red shift of 1.24 nm was observed, meaning the sensitivity of 124 p.m./N. In order to measure the load sensing characteristics of the structure, we gradually increase the longitudinal load strength between ~10 N and ~75 N with a step of ~5 N. As the longitudinal load increasing, the resonant wavelength is red-shifted to a certain degree, which can be clearly observed from the resonant dips in the output spectra of Fig. 6(a). The linear fitting for the wavelength locations as a function of load change was illustrated in Fig. 6(b). It was found that with the increase of the longitudinal load, there are two different ranges can be significantly distinguished in the fitting line with the different sensitivities of 94.5 p.m./N and 46.9 p.m./N, respectively in the sub-ranges of 10–45 N and 50–75 N. The sensitivity difference between the two ranges can be contributed to the reduced FSR and the elastic property of PDMS. The corresponding fitting functions are $\lambda_F = 1583.113 + 0.0945\,F$ and $\lambda_F = 1586.768 + 0.0469\,F$, respectively, with the corresponding resolution of $(0.02\,nm \times 1\,N)/0.0945\,nm = 0.21\,N$ and $(0.02\,nm \times 1\,N)/0.0469\,nm = 0.43\,N$, respectively, depending on the resolution of OSA (0.02 nm). The longitudinal load was known as 2.32×10^3 με/N, and the corresponding sensitivity was 0.041 p.m./με. The working range is seriously limited by the small FSR and the tensile limit of PDMS film. These two factors were determined by the MKR size and PDMS thickness, respectively. The proposed sensor probe was used to measure the longitudinal load. But for most of fiber strain sensors, the stretch force response along the fiber was studied [31–33]. Therefore, the sensitivities cannot be compared with each other. To reveal the stability and repeatability of the proposed load prone, the resonant wavelength was compared when the longitudinal load decreased from ~75 N to ~10 N. The resonant wavelength underwent a red shift back to the original wavelength with a different value of less than 20 p.m. after 52 circles. The poor repeatability is mainly due to the elastic deformation characteristics and packaging process of PDMS materials.

When the longitudinal load is applied onto the sensor probe, the elasto–optical effect will deform the PDMS film, which in turn drives the change of the micro-ring length of MKR structure. To reveal the impact of the micro-ring length on the sensing performance, another PDMS packaged MKR with the microfiber diameter of 6.82 μm and the micro–ring diameter of 5.6 mm was prepared. The sensing performance was also studied under the same experimental conditions. With the increase of longitudinal load, the resonance peak blue–shifted. When the longitudinal load increased from 0 N to 50 N, the resonant wavelength decreased from 1565.93 nm to 1563.88 nm with the longitudinal load sensitivity of 44 p.m./N and the resolution of 0.45 N. Compared with above experimental results, it can be concluded that the larger micro-ring will result in a smaller sensitivity or lower resolution because of its smaller relative change per unit strain. The MKR with different microfiber diameter and ring length have been experimentally studied. The results reveal that the smaller MKR ring length results in higher longitudinal load sensitivity; but the microfiber diameter contributes little.

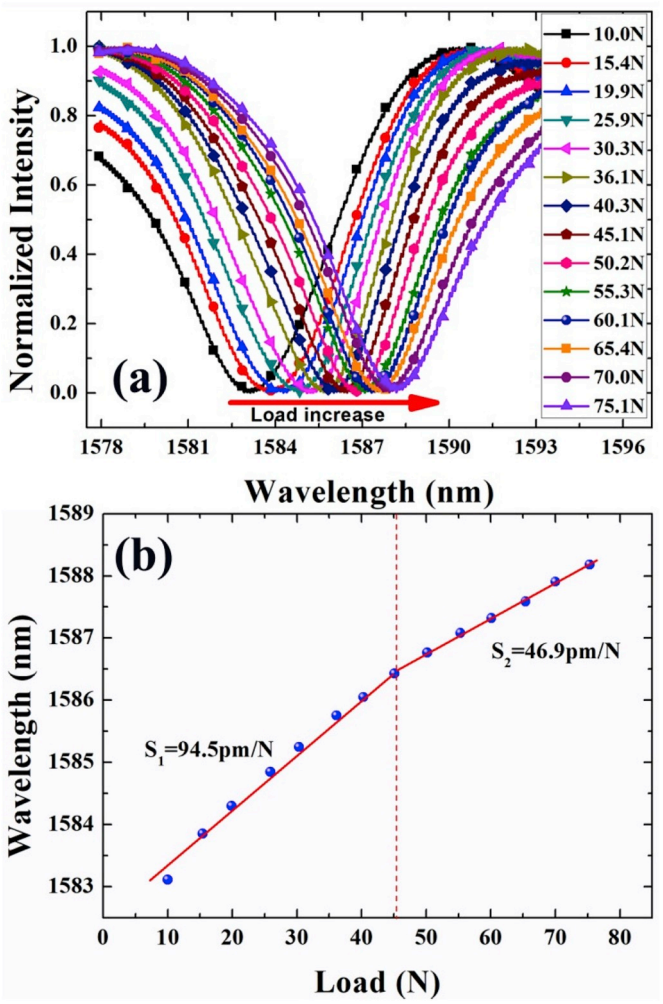

Fig. 6. (a) Spectra and (b) sensing characteristics curve for resonant dip changes as a function of longitudinal load increasing from 10.0 N to 75.1 N.

6. Conclusions

The longitudinal load sensing characteristics of a bare MKR was experimentally demonstrated with a small sensitivity of 6 p.m./N, which is due to the large Young's modulus and low elasto–optical effect of silica materials. In order to improve its sensing sensitivity and probe stability, PDMS material was chosen to encapsulate the bare MKR. With the small Young's modulus, PDMS was easily deformed and used to improve the longitudinal load sensitivity significantly. Furthermore, the large Poisson's ratio enables the conversion of longitudinal load to transverse strain. Therefore, the strain sensitivity can be determined by measuring the longitudinal load. In addition, the excellent physico-chemical properties of PDMS greatly improve the stability of silica MKR

structure. The strain sensing performance of the PDMS packaged MKR was conducted experimentally with the load sensitivity of 94.5 p.m./N, corresponding to the load sensitivity of 0.041 p.m./με.

Declaration of competing interest

The authors declare that they have no known competing financial interests or personal relationships that could have appeared to influence the work reported in this paper.

Acknowledgement

This work was supported by Fundamental Research Funds for the Central Universities (N170405003) and Liaoning Province Natural Science Foundation (number 20180510015).

Appendix A. Supplementary data

Supplementary data to this article can be found online at https://doi.org/10.1016/j.jpcs.2019.109268.

References

[1] N. Gao, Z. Mu, J. Li, Palladium nanoparticles doped polymer microfiber functioned as a hydrogen probe, Int. J. Hydrogen Energy 44 (2019) 14085–14091.
[2] Z.B. Li, Y. Zhang, C.Q. Ren, Z.Q. Sui, J. Li, A high sensitivity temperature sensing probe based on microfiber fabry-perot interference, Sensors 19 (2019) 1819.
[3] J.A. Valles, D. Benedicto, Optimized active muticore fiber bending sensor, Opt. Mater. 87 (2019) 53–57.
[4] L.T. Gai, J. Li, Y. Zhao, Preparation and application of microfiber resonant ring sensors: a review, Opt. Laser. Technol. 89 (2017) 126–136.
[5] M. Sumetsky, Y. Dulashko, J.M. Fini, A. Hale, D.J. DiGiovanni, The microfiber loop resonator: theory, experiment, and application, J. Light. Technol. 24 (2006) 242–250.
[6] K.S. Lim, S.W. Harun, S.S.A. Damanhuri, A.A. Jasim, C.K. Tio, H. Ahmad, Current sensor based on microfiber knot resonator, Sens. Actuators A Phys. 167 (2011) 60–62.
[7] M.S. Boybay, O.M. Ramahi, Material characterization using complementary split-ring resonators, IEEE T. Instrum. Meas. 61 (2012) 3039–3046.
[8] H.J. Yang, S.S. Wang, X. Wang, Y.P. Liao, J. Wang, Temperature sensing in seawater based on microfiber knot resonator, Sensors 14 (2014) 18515–18525.
[9] J.H. Li, J.H. Chen, S.C. Yan, Y.P. Ruan, F. Xu, Y.Q. Lu, Versatile hybrid plasmonic microfiber knot resonator, Opt. Lett. 42 (2017) 3395–3398.
[10] X. Zeng, Y. Wu, C.L. Hou, J. Bai, G.G. Yang, A temperature sensor based on optical microfiber knot resonator, Opt. Commun. 282 (2009) 3817–3819.
[11] Y. Wu, Y.J. Rao, Y.H. Chen, Y. Gong, Miniature fiber-optic temperature sensors based on silica/polymer microfiber knot resonators, Opt. Express 17 (2009) 18142–18147.
[12] H. Yu, L. Xiong, Z. Chen, Q.G. Li, X.N. Yi, Y. Ding, F. Wang, H. Lv, Y.M. Ding, Solution concentration and refractive index sensing based on polymer microfiber knot resonator, APEX 7 (2014) 343–352.
[13] Z.L. Xu, Q.Z. Sun, B.R. Li, Y.Y. Luo, W.G. Lu, D.M. Liu, P.P. Shum, L. Zhang, Highly sensitive refractive index sensor based on cascaded microfiber knots with Vernier effect, Opt. Express 23 (2015) 6662–6672.
[14] Y. Wu, T.H. Zhang, Y.J. Rao, Y. Gong, Miniature interferometric humidity sensors based on silica/polymer microfiber knot resonators, Sens. Actuators B Chem. 155 (2011) 258–263.
[15] H. Ahmad, M.T. Rahman, S.N.A. Sakeh, M.Z.A. Razak, M.Z. Zulkifli, Humidity sensor based on microfiber resonator with reduced graphene oxide, Optik: International Journal for Light and Electron Optics 127 (2016) 3158–3161.
[16] K.S. Lim, Y.S. Chiam, S.W. Phang, W.Y. Chong, C.H. Pua, A.Z. Zulkifli, I. Ganesan, S.W. Harun, H. Ahmad, A Polyaniline–coated integrated microfiber resonator for UV detection, IEEE Sens. J. 13 (2013) 2020–2025.
[17] A. Sulaiman, S.W. Harun, F. Ahmad, S.F. Norizan, H. Ahmad, Electrically tunable microfiber knot resonator based erbium-doped fiber laser, IEEE J. Quantum Electron. 48 (2012) 443–446.
[18] S.C. Yan, B.C. Zheng, J.H. Chen, F. Xu, Y.Q. Lu, Optical electrical current sensor utilizing a graphene-microfiber-integrated coil resonator, Appl. Phys. Lett. 107 (2015) 57.
[19] J.H. Li, F. Xu, Y.P. Ruan, A hybrid plasmonic microfiber knot resonator and mechanical applications, in: 16th International Conference on Optical Communications and Networks (ICOCN), 2017, pp. 1–3. August).
[20] Y. Wu, X. Zeng, Y.J. Rao, Y. Gong, C.L. Hou, G.G. Yang, MOEMS accelerometer based on microfiber knot resonator, IEEE Photonics Technol. Lett. 21 (2009) 1547–1549.
[21] J.M. De Freitas, T.A. Birks, M. Rollings, Optical micro-knot resonator hydrophone, Opt. Express 23 (2015) 5850–5860.
[22] J. Li, L.T. Gai, H.Y. Li, H.F. Hu, A high sensitivity temperature sensor based on packaged microfiber knot resonator, Sens. Actuators A Phys. 263 (2017) 369–372.
[23] R. Fan, Z.Z. Mu, J. Li, Miniature temperature sensor based on polymer-packaged silica microfiber resonator, J. Phys. Chem. Solids 129 (2019) 307–311, 2019.
[24] J. Li, J.T. Yang, J.N. Ma, Load sensing of a microfiber knot ring (MKR) encapsulated in polydimethylsiloxane (PDMS), Instrum. Sci. Technol. 47 (2019) 511–521.
[25] W.S. Lee, K.S. Yeo, A. Andriyana, Y.G. Shee, F.M. Adikan, Effect of cyclic compression and curing agent concentration on the stabilization of mechanical properties of PDMS elastomer, Mater. Des. 96 (2016) 470–475.
[26] R.B. Wagreich, W.A. Atia, H. Singh, J.S. Sirkis, Effects of diametric load on fibre Bragg gratings fabricated in low birefringent fibre, Electron. Lett. 32 (1996) 1223–1224.
[27] Y. Du, Y. Chen, Y. Zhuang, C. Zhu, F. Tang, J. Huang, Probing nanostrain via a mechanically designed optical fiber interferometer, IEEE Photonics Technol. Lett. 29 (2017) 1348–1351.
[28] W. Lou, F. Shentu, Y. Wang, C. Shen, X. Dong, Transverse load sensor based on Mach-Zehnder interferometer constructed by a bowknot type taper, Opt. Fiber Technol. 40 (2018) 52–55.
[29] Y. Wu, B. Liu, J. Wu, L. Zhao, T. Sun, Y. Mao, J. Wang, A transverse load sensor with ultra-sensitivity employing Vernier-effect improved parallel-structured fiber-optic Fabry-Perot interferometer, IEEE Access 7 (2019) 120297–120303.
[30] A.D. Gomes, O. Frazão, Microfiber knot with taper interferometer for temperature and refractive index discrimination, IEEE Photonics Technol. Lett. 29 (2017) 1517–1520.
[31] J. Tian, S. Liu, W. Yu, P. Deng, Microfiber Bragg grating for temperature and strain sensing applications, Photonic Sensors 7 (2017) 44–47.
[32] Y.G. Han, Temperature-insensitive strain measurement using a birefringent interferometer based on a polarization-maintaining photonic crystal fiber, Appl. Phys. B 95 (2009) 383–387.
[33] G.K. Costa, P.M. Gouvêa, L.M. Soares, J.M. Pereira, F. Favero, A.M. Braga, P. Palffy-Muhoray, A.C. Bruno, I.C. Carvalho, In-fiber Fabry-Perot interferometer for strain and magnetic field sensing, Opt. Express 24 (2016) 14690–14696.